Facilitating Dynamic Balance Recovery in Lower-Limb Exoskeletons with State Estimation

Keaton Inkol, John McPhee

Systems Design Engineering
University of Waterloo
200 University Ave W, N2L 3G1, Waterloo, Canada
[kainkol, mcphee]@uwaterloo.ca

EXTENDED ABSTRACT

1 Introduction

Due to their exciting prospects, wearable robotic exoskeletons are seeing increased interest from both lay and scientific communities, though they are limited in their capabilities, e.g., difficult to remain balanced in [1]. Often, it is advantageous to use an underlying multibody dynamic model to inform the control decisions for these devices [2]. However, controls can be difficult in cases with limited onboard sensors. Likewise, hardware limitations like signal quantization also pose challenges for efficient controls. State estimation techniques can remedy this issue by utilizing the same multibody model that is used for controls.

In many existing exoskeletons, the actuators have been designed with high ratio gearing, e.g., strain wave gearing. While these make the onboard electric actuators capable of greater torque generation, they also cause two major issues: i) rotor and gear inertia are reflected back to the end user; ii) losses due to friction between gearing elements are introduced. Adequate friction compensation is a further challenge as friction coefficients are challenging to determine without careful investigation. These coefficients are subject to change with variations in lubrication, temperature, etc.

The goals of this simulation study are to establish a proof-of-concept for state estimation in lower-limb exoskeletons using multibody dynamics and quantized joint position measurements. Automated balance recovery with the presence of actuator static friction was replicated herein to test the proposed estimator [3].

2 Multibody Dynamic Model of Human-Exoskeleton Standing with State Estimation

The model of standing balance used is an extension of a model published previously [1, 3]. Briefly, human upright standing in the sagittal plane was represented using a compound inverted pendulum with three degrees of freedom as shown in Figure (1): $\mathbf{q} = \{q_{\text{hip}}, q_{\text{knee}}, q_{\text{ankle}}\}^T$. The multibody ordinary differential equations are written in state-space form as follows,

$$\begin{Bmatrix} \dot{\mathbf{q}} \\ \ddot{\mathbf{q}} \end{Bmatrix} = \begin{Bmatrix} \mathbf{v} \\ \mathbf{M}(\mathbf{q})^{-1}(\boldsymbol{\Gamma}(\mathbf{q},\mathbf{v}) + \boldsymbol{\tau}(\mathbf{v},\mathbf{u})) \end{Bmatrix} = \dot{\mathbf{x}} = \mathbf{f}(\mathbf{x}, \boldsymbol{\tau}(\mathbf{x},\mathbf{u})) \tag{1}$$

where $\mathbf{M}$ is the mass matrix, $\boldsymbol{\Gamma}$ contains gravitational and velocity-dependent torques, and $\boldsymbol{\tau}$ are resultant joint torques. Human segment inertial parameters were estimated according to the user height and weight (1.80 m, 75 kg) using anthropometric data from the literature [1]. Exoskeleton linkage and reflected actuator inertia were estimated from the Technaid Exo-H3 (Spain) using a combination of physical measurements and CAD analyses [1, 3].

Vector $\mathbf{u} \in \mathbb{R}^3$ are the torques arising from the electric motor only. To include losses due to gearing, a nonlinear continuous velocity-dependent friction model featuring Coulomb torques α_0, breakaway torques $\alpha_0 + \alpha_1$, and a viscous friction coefficient, μ_v, was included,

$$\tau_i(v_i, u_i) = u_i - \alpha_0 \tanh(4\frac{v_i}{v_t}) - \alpha_1 \frac{16 v_i v_t^3}{(v_i^2 + 3v_t^2)^2} - \mu_v v_i \tag{2}$$

where v_t is the transition velocity. Note: α_0 is an important parameter for mimicking “stiction" in strain-wave gearing.

The goal of EKF was to identify the hidden state of the full system given some noisy position measurements $\tilde{q}_k \sim \mathcal{N}(q_k, \mathbf{R})$ taken at instant k (via the extended Kalman filter; EKF [5]). Additionally, we assume that $\tilde{q}_k$ has undergone rounding to the nearest degree. Estimating successive states required computation of the discrete state space Jacobian at each sampling instant:

$$\mathbf{g}_k = \mathbf{x}_k + \delta t \mathbf{f}(\mathbf{x}_k, \boldsymbol{\tau}(\mathbf{x}_k, \mathbf{u}_k)), \quad \mathbf{F}_k = \frac{d\mathbf{g}_k}{d\mathbf{x}} = \mathbf{I} + \delta t \frac{\partial \mathbf{f}}{\partial \mathbf{x}}\bigg|_{\mathbf{x}_k, \mathbf{u}_k} + \delta t \frac{\partial \mathbf{f}}{\partial \boldsymbol{\tau}} \frac{\partial \boldsymbol{\tau}}{\partial \mathbf{x}}\bigg|_{\mathbf{x}_k, \mathbf{u}_k} \tag{3}$$

These derivatives, including those for the friction model, were automatically generated in Maple symbolic computing software. Each successive state estimate was fed back into a linear quadratic regulator (LQR) that assumed actuators were ideal in order to maintain upright stability like a human (torques were saturated at 100 Nm; [3]).

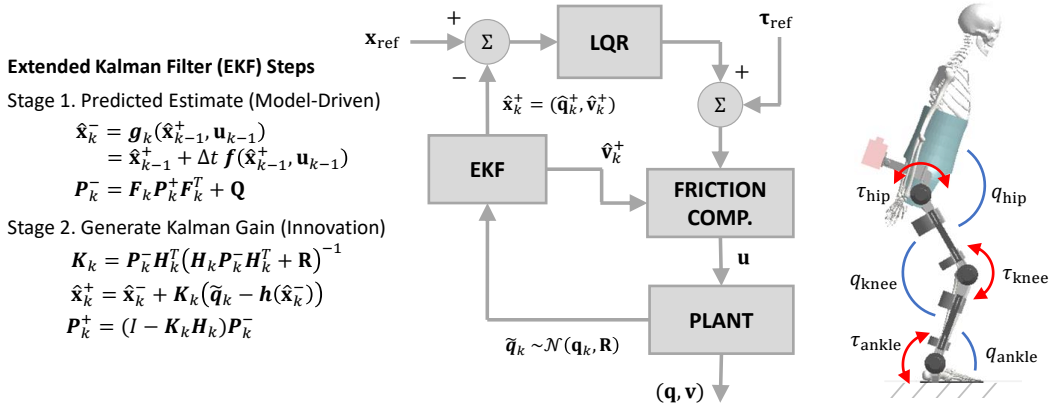

Figure 1: Schematic of the multibody dynamic model and control design with state estimation.

3 Simulation Results and Conclusions

Four test cases were used to test the EKF with limitations imposed: true full-state observations (no EKF) with no plant friction (ideal case; BASE); no friction in plant/EKF (TEST 1); no friction in EKF, but in plant (TEST 2); friction in both EKF and plant (TEST 3). In each simulation, the experiments of Maki and McIlroy [6] were replicated; the floor suddenly translated back with a maximum speed of 30 cm/s over 0.60 s. Friction parameters were set to $\alpha_0 = 3$ Nm, $\alpha_1 = 4$ Nm, $\mu_v = 0.2$ Nm/s, $v_t = 0.001$ m/s.

In each simulation, the exo-assisted “user" never fell and the EKF performed sufficiently for real-time implementation (Figure 2). The EKF and plant without friction (TEST 1) surprisingly struggled with state estimation, especially for the hip velocity ($\hat{\mathbf{v}}^+$ RMSE = 9.5 ± 10.1 deg/s). The result was more pronounced joint displacements than anticipated (especially in the hip). Adding friction to the plant (TEST 2) resulted in closer hip joint trajectories relative to the BASE condition ($\hat{\mathbf{v}}^+$ RMSE = 11.7 ± 3.5 deg/s); however, it also reduced knee mobility and the onset of corrective ankle maneuvers. Adding friction to the EKF (TEST 3) had a marginal effect on the resulting balance control ($\hat{\mathbf{v}}^+$ RMSE = 11.2 ± 3.6 deg/s). These results suggest that the iterative velocity estimates were not accurate enough to compensate for friction such that the ankle and knee actuators behaved as ideal for the LQR. Equation (3) mimics stiction as a high linear damper at $v_i \approx 0$, therefore, the large torque derivative may have prevented ideal Kalman recursion. Further work is necessary to determine whether other state estimation techniques could solve this issue.

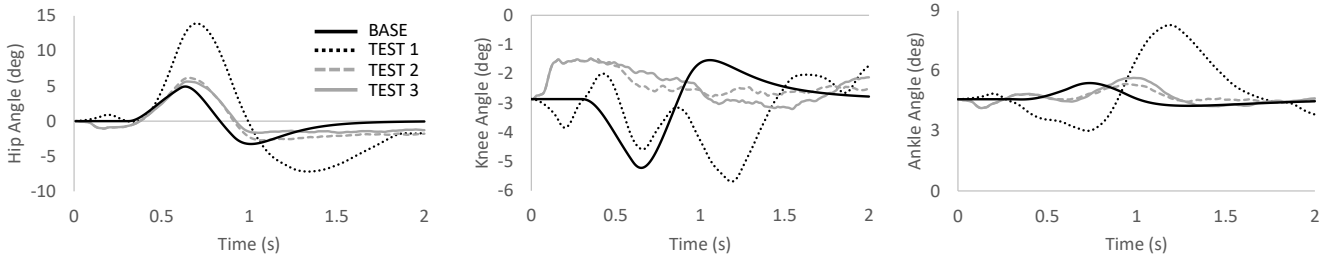

Figure 2: Simulated joint angles (true values; not estimated) for each test case.

References

[1] K. Inkol, J. McPhee. Using Dynamic Simulations to Estimate the Feasible Stability Region of Feet-In-Place Balance Recovery for Lower-Limb Exoskeleton Users. 9th IEEE Conf for Biomed Robotics Biomechatr (BioRob), 1-6, 2022

[2] W.J. Jaimes et al. Modeling and Simulation of a Lower Limb Exoskeleton with Computed Torque Control for Gait Rehabilitation. Global Medical Eng Physics Exchanges/PanAm Health Care Exchanges (GMEPE/PAHCE), 1-6, 2021

[3] K. Inkol, J. McPhee. Assessing Control of Fixed Support Balance Recovery in Wearable Lower-Limb Exoskeletons Using Multibody Dynamic Modelling. 8th IEEE Conf for Biomed Robotics Biomechatr (BioRob), 54-60, 2020

[4] P. Brown, J. McPhee. A Continuous Velocity-Based Friction Model for Dynamics and Control With Physically Meaningful Parameters. ASME Journal of Computational and Nonlinear Dynamics, 11(5):054502, 2016.

[5] D. Simon. Kalman Filtering with State Constraints: A Survey of Linear and Nonlinear Algorithms. IET Control Theory and Applications, 4(8):1303-1318, 2010.

[6] B.E. Maki et al. Influence of lateral destabilization on compensatory stepping responses. Journal of Biomechanics, 29(3):343-353, 1996.